MULTI-TARGET DETECTION WITH THE GENERALIZED METHOD OF MOMENTS

Authors

School of Electrical Engineering, Tel Aviv University, Tel Aviv, Israel

ABSTRACT

The abstract should appear at the top of the left-hand column of text, about 0.5 inch (12 mm) below the title area and no more than 3.125 inches (80 mm) in length. Leave a 0.5 inch (12 mm) space between the end of the abstract and the beginning of the main text. The abstract should contain about 100 to 150 words, and should be identical to the abstract text submitted electronically along with the paper cover sheet. All manuscripts must be in English, printed in black ink.

***Index Terms*—** One, two, three, four, five

1. INTRODUCTION

We study the multi-target detection (MTD) problem of estimating a target signal $x : \{0, \dots, L-1\} \to \mathbb{R}$ from a noisy measurement that contains multiple copies of the signal, each randomly translated [1], [2], [3], [4], [5], [6]. Specifically, let $y : \{0, \dots, N-1\} \to \mathbb{R}$ be a measurement of the form

$$y[\ell] = \sum_{i=1}^{p} x[\ell - \ell_i] + \varepsilon[\ell], \tag{1}$$

where $\{\ell_i\}_{i=1}^{p} \in \{L+1, \dots, N-L\}$ are arbitrary translations, and $\varepsilon[\ell]$ is i.i.d. Gaussian noise with zero mean and variance σ^2.

The translations and the number of occurrences of x in y are unknown. Figure 1 presents an example of a measurement y at different signal-to-noise ratios (SNRs). We define SNR $:= \frac{\|x\|_2^2}{L\sigma^2}$, where L is the length of x (in pixels), and σ^2 is the noise variance.

The MTD model arises in several scientific applications, such as passive radar [7], astronomy [8], motion deblurring [9], and system identification [10]. In particular, it serves as mathematical abstraction of the cryo-electron microscopy (cryo-EM) technology for macromolecular structure determination [11], [12], [13]. In a cryo-EM experiment [14], biological macromolecules suspended in a liquid solution are rapidly frozen into a thin ice layer. An electron beam then passes through the sample, and a two-dimensional tomographic projection is recorded. Importantly, the 2-D location and 3-D orientation of particles within the ice are random and unknown. This measurement, called *micrograph*, is affected by high noise levels and the optical configuration of the microscope. This transformation is typically modeled as a convolution of the model (1) with a point spread function, whose Fourier transform is called contrast transfer function (CTF) [15], [16].

In the current analysis workflow of cryo-EM data [17], [18], [19], the 2-D projections are first detected and extracted from the micrograph, and later rotationally and translationally aligned to reconstruct the 3-D molecular structure. This approach fails for small molecules, which induce low contrast, and thus low SNR. This makes them difficult to detect and align [6], [11], [17], [20], rendering current cryo-EM algorithmic pipeline ineffective. For example, in the limit SNR $\to 0$, reliable detection of signals' locations within the measurement is impossible [6, Proposition 3.1].

The MTD model was devised in [6] in order to study the recovery of small molecules directly from the micrograph, below the current detection limit of cryo-EM [11], [21]. An autocorrelation analysis technique (see Section 2.1) was implemented to recover low-resolution 3-D structures from noiseless simulated data under a simplified model. Autocorrelation analysis consists of finding an image that best explains the empirical autocorrelations of the measurement. For any noise level, those autocorrelations can be estimated to any desired accuracy for sufficiently large N. Computing the autocorrelations is straightforward and requires only one pass over the data, which is advantageous for massively large datasets, such as cryo-EM datasets [17]. As such, autocorrelation analysis provides an attractive alternative to other computational methods, such as maximum likelihood estimation, which is intractable for the MTD problem [2].

2. MATHEMATICAL FRAMEWORK

2.1. Autocorrelation analysis

The autocorrelation of order q of a random signal $z \in \mathbb{R}^N$ is defined as

$$A_z^q[\ell_1, \dots, \ell_{q-1}] := \mathbb{E}_z\Big[\frac{1}{N^2} \sum_{i \in \mathbb{R}^2} z[i] z[i+\ell_1] \cdots z[i+\ell_{q-1}]\Big], \tag{2}$$

S.K. is supported by the Yitzhak and Chaya Weinstein Research Institute for Signal Processing. T.B. is supported in part by NSF-BSF grant no. 2019752, and the Zimin Institute for Engineering Solutions Advancing Better Lives.

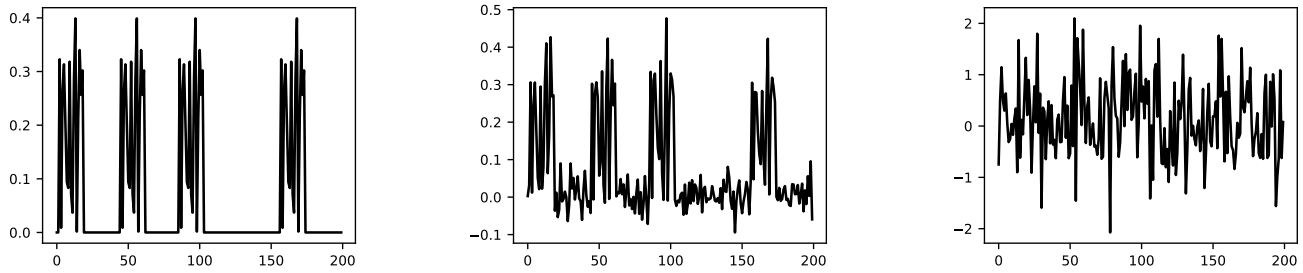

(a) No noise. (b) SNR $= 50$. (c) SNR $= 0.1$.

Fig. 1: Three measurements y from (1) at different noise levels: no noise (left); SNR $= 50$ (middle); SNR $= 0.1$ (right). Each measurement contains multiple copies of the target signal in arbitrary locations. In this work, our goal is to estimate the target signal directly from y. We focus on the low SNR regime (e.g., panel (c)) in which the signal occurrences are swamped by the noise, and the locations of the signal occurrences cannot be detected reliably.

where $\ell_1, \ldots, \ell_{q-1}$ are integer shifts. Indexing out of bounds is zero-padded, that is, $z[i] = 0$ out of the range $\{0, \ldots, N-1\}$. In this work, we use the first three autocorrelations which are explicitly given by

$$A_z^1 = \mathbb{E}_z \left[\frac{1}{N} \sum_{i \in \mathbb{Z}} z\,[i] \right], \tag{3}$$

$$A_z^2\,[\ell] = \mathbb{E}_z \left[\frac{1}{N} \sum_{i \in \mathbb{Z}} z\,[i]\, z\,[i+\ell] \right], \tag{4}$$

$$A_z^3\,[\ell_1, \ell_2] = \mathbb{E}_z \left[\frac{1}{N} \sum_{i \in \mathbb{Z}} z\,[i]\, z\,[i+\ell_1]\, z\,[i+\ell_2] \right]. \tag{5}$$

As N grows indefinitely, the empirical autocorrelations of z almost surely (a.s.) converge to the population autocorrelations of z:

$$\lim_{N \to \infty} \frac{1}{N} \sum_{i \in \mathbb{Z}^2} z[i] z[i+\ell_1] \cdots z[i+\ell_{q-1}] \overset{\text{a.s.}}{=} A_z^q[\ell_1, \ldots, \ell_{q-1}]. \tag{6}$$

Our goal is to relate the autocorrelations of the measurement with the target signal x. In particular, the first-order autocorrelation is defined as

$$A_y^1 := \frac{1}{N} \sum_{i \in \mathbb{Z}} y[i]. \tag{7}$$

This is the mean of the measurement. The second-order autocorrelation of y, $A_y^2 : \mathbb{Z} \to \mathbb{R}$, is defined by

$$A_y^2[\ell_1] := \frac{1}{N} \sum_{i \in \mathbb{Z}} y[i] y[i+\ell_1], \tag{8}$$

and the third-order autocorrelation $A_y^3 : \mathbb{Z} \times \mathbb{Z} \to \mathbb{R}$ by

$$A_y^3[\ell_1, \ell_2] := \frac{1}{N} \sum_{i \in \mathbb{Z}} y[i] y[i+\ell_1] y[i+\ell_2]. \tag{9}$$

2.2. Autocorrelations under the well-separated model

We first discuss the well-separated case of the MTD problem, which was studied in [1]. In this case, we assume that each signal in the measurement y is separated by at least a full signal length from its neighbors. Specifically, we assume that

$$|\ell_{i_1} - \ell_{i_2}| \geq 2L - 1, \quad \text{for all } i_1 \neq i_2. \tag{10}$$

To compute the third-order autocorrelation (9), we compute the product of y with its two shifts. Importantly, for ℓ-s in the range

$$\mathcal{L} = \{0, \ldots, L-1\}, \tag{11}$$

any given occurrence of x in y is only ever correlated with itself, and never with another occurrence.

In [1], it was shown that under the separation condition (10), for any fixed level of noise σ^2, density γ and signal length L, in the limit $N \to \infty$ we have that

$$A_y^1 \overset{\text{a.s.}}{=} \gamma A_x^1, \tag{12}$$

$$A_y^2[\ell_1] \overset{\text{a.s.}}{=} \gamma A_x^2[\ell_1] + \sigma^2 \delta[\ell_1], \tag{13}$$

$$A_y^3[\ell_1, \ell_2] \overset{\text{a.s.}}{=} \gamma A_X[\ell_1, \ell_2] + \gamma S_1 \sigma^2 (\delta[\ell_1] + \delta[\ell_2] + \delta[\ell_1 - \ell_2]), \tag{14}$$

for $\ell_1, \ell_2 \in \mathcal{L}$ (defined in (11)), where

$$\delta[\ell] = \begin{cases} 1 \text{ if } \ell = \vec{0}, \\ 0 \text{ otherwise}, \end{cases} \tag{15}$$

is the Kronecker delta function. Here, γ is the density of the target images in the measurement and is defined by

$$\gamma = p \frac{L}{N}. \tag{16}$$

As such, (12) - (14) relate the autocorrelations of the measurement with those of the target signal x. Moreover,

the signal x can be identified from its autocorrelations, and thus, potentially, also from the autocorrelations of the measurement. In [1], it was shown that γ (respectively σ) can be estimated from the first- and second-order autocorrelations of the measurement if σ (respectively γ) is known. In particular, if γ and σ are known (or are reliably estimated), we can provably determine the signal from the measurement's autocorrelations. Previous works [1], [2], [3], [4], [5] demonstrated successful signal and image estimations. Importantly, the aforementioned relations between the autocorrelations of M and F do not directly depend on the location of individual signal occurrences in the measurement, but only through the density parameter γ. Therefore, detecting the signal occurrences is not a prerequisite for signal recovery, and thus signal recovery is possible even in very low SNR regimes.

2.3. Signal recovery from autocorrelations

2.4. Generalized method of moments

3. NUMERICAL EXPERIMENTS

The paper title (on the first page) should begin 1.38 inches (35 mm) from the top edge of the page, centered, completely capitalized, and in Times 14-point, boldface type. The authors' name(s) and affiliation(s) appear below the title in capital and lower case letters. Papers with multiple authors and affiliations may require two or more lines for this information. Please note that papers should not be submitted blind; include the authors' names on the PDF.

4. CONCLUSION

5. REFERENCES

[1] Tamir Bendory, Nicolas Boumal, William Leeb, Eitan Levin, and Amit Singer, "Multi-target detection with application to cryo-electron microscopy," *Inverse Problems*, vol. 35, no. 10, pp. 104003, 2019.

[2] Ti-Yen Lan, Tamir Bendory, Nicolas Boumal, and Amit Singer, "Multi-target detection with an arbitrary spacing distribution," *IEEE Transactions on Signal Processing*, vol. 68, pp. 1589–1601, 2020.

[3] Nicholas F Marshall, Ti-Yen Lan, Tamir Bendory, and Amit Singer, "Image recovery from rotational and translational invariants," in *ICASSP 2020-2020 IEEE International Conference on Acoustics, Speech and Signal Processing (ICASSP)*. IEEE, 2020, pp. 5780–5784.

[4] Tamir Bendory, Ti-Yen Lan, Nicholas F Marshall, Iris Rukshin, and Amit Singer, "Multi-target detection with rotations," *arXiv preprint arXiv:2101.07709*, 2021.

[5] Shay Kreymer and Tamir Bendory, "Two-dimensional multi-target detection," *arXiv preprint arXiv:2105.06765*, 2021.

[6] Tamir Bendory, Nicolas Boumal, William Leeb, Eitan Levin, and Amit Singer, "Toward single particle reconstruction without particle picking: breaking the detection limit," *arXiv preprint arXiv:1810.00226*, 2018.

[7] Sandeep Gogineni, Pawan Setlur, Muralidhar Rangaswamy, and Raj Rao Nadakuditi, "Passive radar detection with noisy reference channel using principal subspace similarity," *IEEE Transactions on Aerospace and Electronic Systems*, vol. 54, no. 1, pp. 18–36, 2017.

[8] Timothy J Schulz, "Multiframe blind deconvolution of astronomical images," *JOSA A*, vol. 10, no. 5, pp. 1064–1073, 1993.

[9] Anat Levin, "Blind motion deblurring using image statistics," *Advances in Neural Information Processing Systems*, vol. 19, pp. 841–848, 2006.

[10] Karim Abed-Meraim, Wanzhi Qiu, and Yingbo Hua, "Blind system identification," *Proceedings of the IEEE*, vol. 85, no. 8, pp. 1310–1322, 1997.

[11] Richard Henderson, "The potential and limitations of neutrons, electrons and X-rays for atomic resolution microscopy of unstained biological molecules," *Quarterly Reviews of Biophysics*, vol. 28, no. 2, pp. 171–193, 1995.

[12] Eva Nogales, "The development of cryo-EM into a mainstream structural biology technique," *Nature methods*, vol. 13, no. 1, pp. 24–27, 2016.

[13] Xiao-Chen Bai, Greg McMullan, and Sjors HW Scheres, "How cryo-EM is revolutionizing structural biology," *Trends in Biochemical Sciences*, vol. 40, no. 1, pp. 49–57, 2015.

[14] Joachim Frank, *Three-dimensional electron microscopy of macromolecular assemblies: visualization of biological molecules in their native state*, Oxford University Press, 2006.

[15] Ayelet Heimowitz, Joakim Andén, and Amit Singer, "Reducing bias and variance for CTF estimation in single particle cryo-EM," *Ultramicroscopy*, vol. 212, pp. 112950, 2020.

[16] HP Erickson and Aaron Klug, "Measurement and compensation of defocusing and aberrations by Fourier processing of electron micrographs," *Philosophical Transactions of the Royal Society of London. B, Biological Sciences*, vol. 261, no. 837, pp. 105–118, 1971.

[17] Tamir Bendory, Alberto Bartesaghi, and Amit Singer, "Single-particle cryo-electron microscopy: Mathematical theory, computational challenges, and opportunities," *IEEE Signal Processing Magazine*, vol. 37, no. 2, pp. 58–76, 2020.

[18] Sjors HW Scheres, "RELION: implementation of a Bayesian approach to cryo-EM structure determination," *Journal of Structural Biology*, vol. 180, no. 3, pp. 519–530, 2012.

[19] Ali Punjani, John L Rubinstein, David J Fleet, and Marcus A Brubaker, "cryoSPARC: algorithms for rapid unsupervised cryo-EM structure determination," *Nature methods*, vol. 14, no. 3, pp. 290–296, 2017.

[20] Cecilia Aguerrebere, Mauricio Delbracio, Alberto Bartesaghi, and Guillermo Sapiro, "Fundamental limits in multi-image alignment," *IEEE Transactions on Signal Processing*, vol. 64, no. 21, pp. 5707–5722, 2016.

[21] Edoardo D'Imprima and Werner Kühlbrandt, "Current limitations to high-resolution structure determination by single-particle cryoEM," *Quarterly Reviews of Biophysics*, vol. 54, 2021.